

Further analysis of target strength measurements of Antarctic krill at 38 and 120 kHz: Comparison with deformed cylinder model and inference of orientation distribution

Dezhang Chu

Department of Applied Ocean Physics and Engineering, Woods Hole Oceanographic Institution, Woods Hole, Massachusetts 02543

Kenneth G. Foote

Institute of Marine Research, 5024 Bergen, Norway

Timothy K. Stanton

Department of Applied Ocean Physics and Engineering, Woods Hole Oceanographic Institution, Woods Hole, Massachusetts 02534

(Received 18 September 1992; accepted for publication 17 December 1992)

Data collected during the krill target strength experiment [J. Acoust. Soc. Am. **87**, 16–24 (1990)] are examined in the light of a recent zooplankton scattering model where the elongated animals are modeled as deformed finite cylinders [J. Acoust. Soc. Am. **86**, 691–705 (1989)]. Exercise of the model under assumption of an orientation distribution allows absolute predictions of target strength to be made at each frequency. By requiring that the difference between predicted and measured target strengths be a minimum in a least-squares sense, it is possible to infer the orientation distribution. This useful biological quantity was not obtainable in the previous analysis which involved the sphere scattering model.

PACS numbers: 43.30.Xm, 43.30.Ft, 43.30.Gv

INTRODUCTION

In a previous paper, an attempt was made to determine average backscattering cross sections of krill through an analysis of echo data gathered on aggregations of engaged animals.¹ The measured quantities agreed at best very roughly with computations based on a spherical model.² Some differences were significant. These were attributed, at least in part, to neglect of the shape of the animals. Concurrent with the research leading up to that paper was the development of the deformed cylinder model that comes closer to accounting for the shape of the animal.³

Understanding the scattering processes not only allows scattering predictions to be made from knowledge of the animal size, shape, orientation, and material properties, but also allows echo sounders to be used as remote sensing tools to infer some of the above properties. In the case of fish, it has been possible to infer the orientation distribution from measurements of single-scatterer target strength from model calculations based on knowledge of swimbladder morphometry.⁴ The zooplankton scatter data presented in Ref. 1 represent the first substantial set of controlled data from which one can begin to make inferences of orientation. Because of the recent development and success of the deformed cylinder model with other very limited sets of zooplankton data, the general importance of understanding the animals' scattering characteristics, and the importance to biologists in remotely and noninvasively determining animal behavior, the data in Ref. 1 are reanalyzed in this letter in terms of the deformed cylinder model. Specifically, absolute levels predicted by the model are compared with the data, and a technique is developed

and used which allows parameters characterizing the orientation distribution, namely, the mean and standard deviation, to be inferred from the data.

I. DATA

The basic data consist of concurrent measurements of the mean volume backscattering coefficient s_v of live engaged krill at 38 and 120 kHz. Each datum represents the average of about 150 measurements made over a 6-min interval. According to the analysis in Ref. 1, it is possible to express the data from individual measurement series as a paired time series of mean target strength,

$$TS = 10 \log \bar{\sigma} / 4\pi = 10 \log \bar{\sigma}_{bs},$$

where the averaging is done in the σ domain. An example of the time series is presented in Fig. 1(a) and (b).

II. MODEL

The scattering model is that of the deformed fluid-like cylinder,³ with physical parameters close to those of seawater. In order to extend the range of orientations over which the calculations are valid, the far-field backscattering amplitude is evaluated by the distorted-wave Born approximation (DWBA) rather than by the approximate modal-series-based solution given in Ref. 3. In brief, the DWBA expresses the amplitude by an integral over the volume of the scatterer, in which the immersion-medium wave vector of the ordinary Born approximation⁵ is replaced by the internal wave vector in the integration volume. The DWBA scattering amplitude is adapted from Eq. 8.1.20 of Ref. 5 as

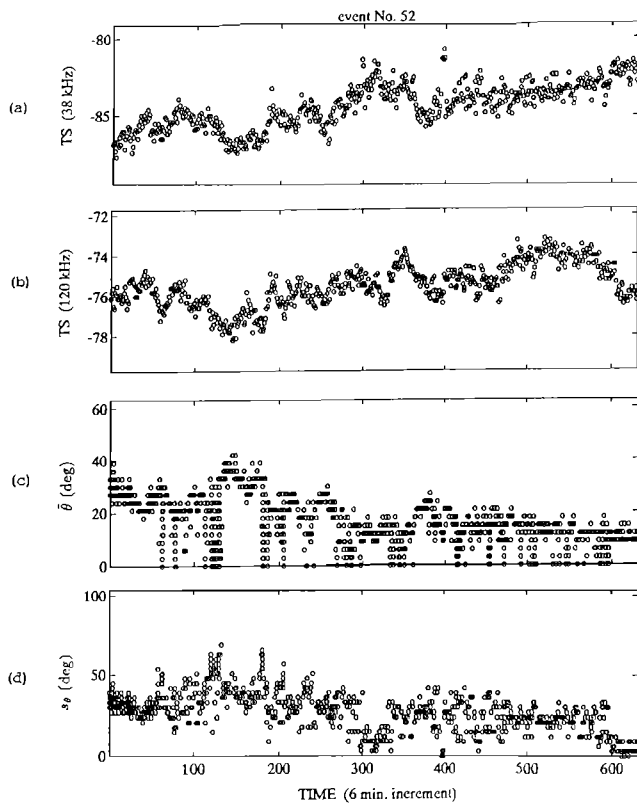


FIG. 1. Time series of single-krill target strength TS at 38 and 120 kHz derived from measurement series 52 of the krill target strength experiment [(a) and (b)] and corresponding time series of candidate solutions for the mean tilt angle $\bar{\theta}$ and standard deviations s_{θ} [(c) and (d)]. Each sample in (a) and (b) represents the result of averaging σ over about 150 echoes collected over a 6-min interval. The data derived from measurement series 52 may be regarded as representative of the majority. The large number of krill of mean length 38.4 mm evidently guarantees a good SNR, as the transitions between candidate solutions are relatively smooth.

$$f = \frac{k^2}{4\pi} \int \int \int_{v_0} (\gamma_{\kappa} + \gamma_{\rho} \cos \phi) e^{i\mu \cdot \mathbf{r}_0} dv_0,$$

TABLE I. Several characteristics of data gathered in the krill target strength experiment: N denotes the number of krill in the cage, with volume 0.104 m^3 ; \bar{l} , the mean total length; n_s , the number of paired samples, each of which represents the result of averaging σ over about 150 pings gathered over a six-minute interval; av and s.d. apply to minimum value of the error quantity E over all n_s samples in each measurement series.

Series number	N	\bar{l} (mm)	Duration	n_s	E_{\min} (dB)	
					av	s.d.
17	496	39.4	16 h 46 m	159	0.29	0.20
19	246	31.8	15 h 22 m	132	2.53	0.71
20	351	33.8	23 h 16 m	206	0.72	0.40
26	752	30.9	23 h 1 m	202	0.29	0.19
28	390	30.1	38 h 38 m	189	2.30	0.65
30	458	35.3	40 h 13 m	376	0.27	0.24
36	1368	32.2	42 h 31 m	424	0.58	0.41
37	787	31.2	18 h 13 m	180	0.29	0.22
43	398	33.5	37 h 3 m	164	0.20	0.17
47	1593	32.8	64 h 41 m	298	0.40	0.18
50	850	31.5	42 h 36 m	232	0.73	0.29
52	816	38.4	65 h 5 m	632	0.35	0.27
55	794	31.3	46 h 7 m	459	0.41	0.20

where k is the wave number of the surrounding fluid, $\gamma_{\kappa} = (\kappa_2 - \kappa_1)/\kappa_1$, $\gamma_{\rho} = (\rho_2 - \rho_1)/\rho_1$, $\kappa = (\rho c^2)^{-1}$ (compressibility), $c = \text{speed of sound}$, $\rho = \text{mass density}$, subscripts "1" and "2" refer to surrounding and body medium, respectively, $\mu = \mathbf{k}_i - \mathbf{k}_s$, \mathbf{k}_i and \mathbf{k}_s are the incident and scattered wave vectors *evaluated in the body medium* ("2"), \mathbf{r}_0 is the position vector, and v_0 is the volume of the body. This integral is evaluated numerically by integrating over the body of the target, taking into account the material properties and scattering geometry, hence source and receiver location, shape and orientation of body. Each target is a uniformly bent, finite-length cylinder, whose cross-sectional radius is essentially uniform over most of the length. To better replicate the shape of the animals, there is slight tapering, which is incorporated in the model by using a variable radius $a = a_0 \{1 - [z/(l/2)]^{10}\}^{1/2}$, where a_0 is the radius at the midsection, z is the position along the axis with $z=0$ corresponding to the midsection, and l is the length.

The sound speed and density contrasts (relative to the surrounding medium) were measured at the time of the experiment to be 1.0279 and 1.0357 (Refs. 6 and 1, respectively). Other scatterer properties are morphometric. The radius of the deformed cylinder representing a single krill is assumed to be $l/16$, where l is the total length of the animal, defined as the distance from the anterior end of the eye to the tip of the telson. The degree of bend of the animal's central axis is characterized by the radius of curvature, which is assumed to be $3l$. Although there is reasonable basis for the choice of this value of radius, the model, once averaged over a distribution of angles of orientation, is insensitive to variations in this for radii greater than l (Ref. 7). The total krill length is specified in Ref. 1 for each measurement series, and is stated here in Table I.

For krill measurement by directional, vertical echo sounders, as in the experiment, the most important component of orientation, and the only one considered here, is the tilt angle θ . This is defined as the angle between the line connecting the end points of the bent cylinder and the horizontal plane. Positive angles are associated with the

head-up orientation, and negative angles, with the head-down attitude. The model in this analysis does not distinguish between these, however, as σ is symmetrical in θ . Head-up orientations may be assumed, at least in the mean, following the observations of Kils,⁸ among others.

Computed values of σ are averaged with respect to normal distributions of θ truncated at two standard deviations s_θ from the mean $\bar{\theta}$. Averaging is also performed with respect to a normal distribution of l that is similarly truncated at two standard deviations Δl from the mean, \bar{l} , where $\Delta l = 0.1\bar{l}$ according to Ref. 1.

III. METHOD

The model has been used to compute σ for each krill length distribution at each of the two frequencies, 38 and 120 kHz, for each of a number of theoretical orientation distributions. The parameter ranges of these are the following: $\bar{\theta}$ spans the range from 0 to 90 deg in steps of 3 deg, while s_θ independently spans the same range.

In order to match predictions of mean target strength TS with measurements, an error quantity E is defined:

$$E = [(TS_1 - \widehat{TS}_1)^2 + (TS_2 - \widehat{TS}_2)^2]^{1/2},$$

where TS_m denotes the predicted TS at the m th frequency and \widehat{TS}_m denotes the corresponding measured value. All pairs of orientation parameters $(\bar{\theta}, s_\theta)$ with computed E values that lie within 10% of the lowest value of E for the same measurement pair $(\widehat{TS}_1, \widehat{TS}_2)$ are selected as candidate solutions.

IV. RESULTS

An example of some least-square determinations of orientation parameters is presented in Fig. 1(c) and (d). Because of inherent ambiguities in the solution, the example does not indicate the precise pairing of values of $\bar{\theta}$ and s_θ , except in trivial, unique instances. Fits between theory and experiment for the entire data set are summarized in Fig. 2, which was generated for direct comparison with Fig. 1 of Ref. 1. The horizontal and vertical bars in Fig. 2(a) are not error bars but rather extreme values obtained in the fitting process for a given measurement series. Because the values on any pair of vertical and horizontal bars are correlated with each other, hence producing a distorted view of the comparison, Fig. 2(b) was drawn to plot individual data from every 6-min interval. The distribution of accepted combinations of $\bar{\theta}$ and s_θ for the whole data set, is presented in Fig. 3.

Predictions of $(\bar{\theta}, s_\theta)$ pairs are weighted in the following manner. For the i th measurement pair $(\widehat{TS}_1, \widehat{TS}_2)_i$, the number of candidate solutions $(\bar{\theta}, s_\theta)_{ij}$ with respective predictions $(TS_1, TS_2)_{ij}$ satisfying the minimization criterion is assumed to be n_i . If the corresponding minimum E value is denoted E_i , then the weight assigned to the j th solution for the i th measurement pair is

$$w_{ij} = n_i^{-1} E_i^{-1} / \sum_{k=1}^n E_k^{-1},$$

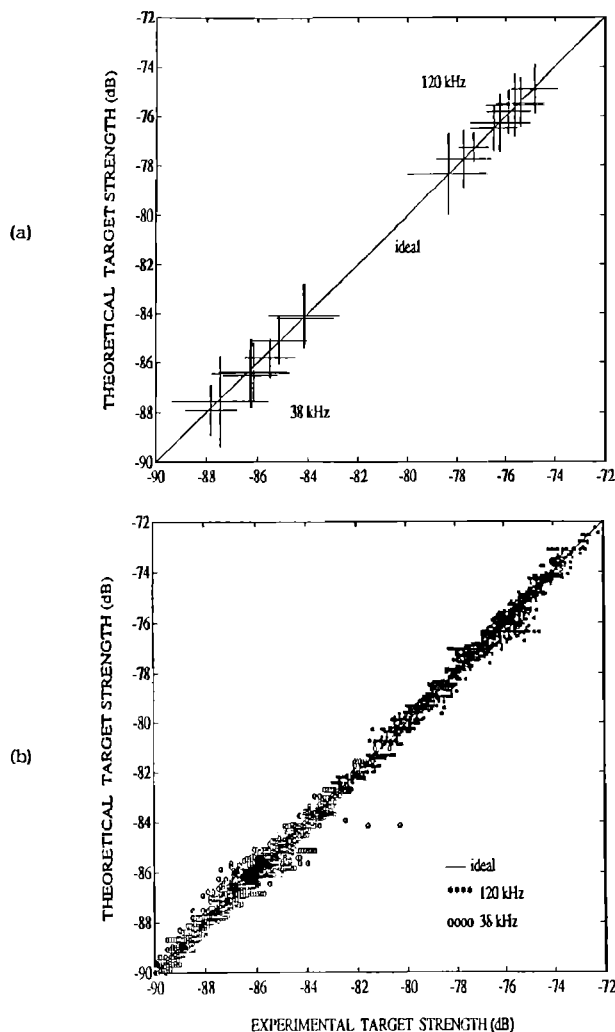


FIG. 2. Comparison between data and theoretical TS determined by best fit to data. The bars in (a) indicate range of values achieved for the many 6-min intervals in each measurement series, i.e., they are not error bars, as the vertical and horizontal values are correlated. This plot was generated for direct comparison with Fig. 1 of Ref. 1. The points in (b) represent the actual values for the 6-min intervals. Both plots show a marked improvement over the comparison between the data and the sphere model in Fig. 1 of Ref. 1.

where n denotes the total number of measurements. This scheme thus assigns equal weights to each of the n_i candidate solutions for the same measurement pair and an overall weighting factor proportional to E_i^{-1} relative to all n classes. The overall agreement of measured and predicted TS values is suggested by the mean, $n^{-1} \sum_{i=1}^n E_i$, for each measurement series. This is included in Table I.

V. DISCUSSION

The fit between the cylinder model and data in Fig. 2 is much closer than that between the sphere model and data in Fig. 1 of Ref. 1, where predictions generally exceed the corresponding measurements, especially at lower values. The improvement suggests promise in the use of the cylinder model with elongated zooplankton. The resultant inferred orientation parameters lie within reasonable

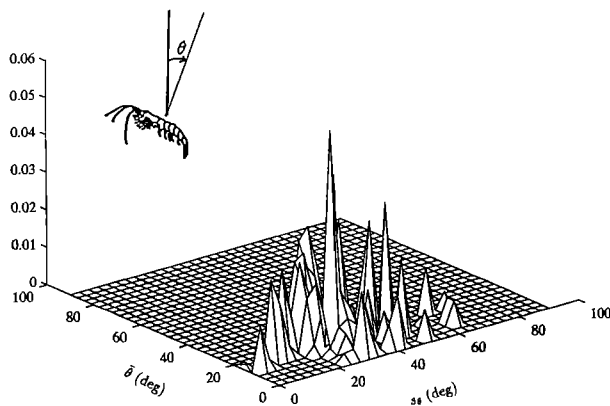


FIG. 3. Frequency distribution of pairs of orientation parameters ($\bar{\theta}, s_{\theta}$) for measurement series 52, also analyzed in Fig. 1. Each value is represented by a pyramid. The range of behavior shown in this plot is broadly consistent with the behavior of other krill summarized in Ref. 8.

bounds and are broadly consistent with the orientation distribution observed by Kils⁸ ($10^{\circ} \leq \bar{\theta} < 30^{\circ}$ for swimming Antarctic krill).

The admitted shortcoming of the target strength experiment is the absence of photographic measurements of orientation. The present model computations consequently cannot be verified by reference to independent measurements, although the model did reject data with a low signal-to-noise ratio, due to a combination of small animal size and low number density. The same lack of photographic observations also applies, strictly speaking, to the predictions of fish orientation made in Ref. 4, although supported by an earlier study on a different species of fish.⁹

Some notable similarities of the new work on zooplankton and older work on fish may be emphasized. Both scattering models are absolute in the sense of making absolute predictions of target strength from an animal of particular morphometry and composition in fixed orientation, when insonified at a given frequency. Both models give plausible predictions of orientation, as judged by experimental data on orientation, although derived in entirely separate experiments. The fact that the zooplankton scattering model rejects the measurement series with the theoretically lowest SNRs gives further confidence in the model, as well as in the majority of the original measurement series, for which the agreement between measurement and prediction is close.

Given the requirement of measurements performed at sufficient SNR, the greatest obstacle to be overcome in determining the parameters of the tilt angle distribution is that of ambiguity. The amount of information available in two-frequency measurements is marginally adequate for this determination.

For applications to field work, measurement of single-scatterer target strength cannot be assumed. What is determined from measurements of the volume scattering

strength is the product of backscattering cross section and the unknown number density of animals. Measurements at three or more suitable frequencies are probably necessary to yield a nonunique determination of the orientation distribution. Admittedly, however, questions of necessity and sufficiency are open.

VI. CONCLUSION

Use of the deformed cylinder model provides fits to the krill scattering data superior to those previously obtained involving the sphere model. The source of the improvement lies in the fact that the cylinder model takes into account the elongation and orientation distribution of this elongated species. One benefit of these fits is an inference of orientation distribution.

It is appreciated that the target strength data, model, and correctness of model parameters may each be wanting. At the least, an essential ingredient of future experiments must be measurement of the orientation distribution. If this were to be measured concurrently with the echo energy, as in the manner of the fish measurements reported in Ref. 9, three distinct gains may be anticipated. These are (1) increased knowledge of target strength through association of this with the orientation distribution, (2) more rigorous verification of scattering models, and (3) improved knowledge of model parameters.

ACKNOWLEDGMENTS

One of us (KF) wishes to express his appreciation to Woods Hole Oceanographic Institution for its invitation to visit in the summer 1992. This research was supported, in part, by the Ocean Acoustics and Oceanic Biology Program of the Office of Naval Research Grant No. N00014-89-J-1729. This is Woods Hole Oceanographic Institution Contribution No. 8108.

¹K. G. Foote, I. Everson, J. L. Watkins, and D. G. Bone, "Target strengths of Antarctic krill (*Euphausia superba*) at 38 and 120 kHz," *J. Acoust. Soc. Am.* **87**, 16-24 (1990).

²C. F. Greenlaw, "Acoustical estimation of zooplankton populations," *Limnol. Oceanogr.* **24**, 226-242 (1979).

³T. K. Stanton, "Sound scattering by cylinders of finite length. III. Deformed cylinders," *J. Acoust. Soc. Am.* **86**, 691-705 (1989).

⁴K. G. Foote and J. J. Traynor, "Comparison of walleye pollock target strength estimates determined from *in situ* measurements and calculations based on swimbladder form," *J. Acoust. Soc. Am.* **83**, 9-17 (1988).

⁵P. M. Morse and U. Ingard, *Theoretical Acoustics* (McGraw-Hill, New York, 1968).

⁶K. G. Foote, "Speed of sound in *Euphausia superba*," *J. Acoust. Soc. Am.* **87**, 1405-1408 (1990).

⁷T. K. Stanton, D. Chu, P. H. Wiebe, and C. S. Clay, "Average echoes from randomly oriented random-length finite cylinders: Zooplankton models," submitted to *J. Acoust. Soc. Am.*

⁸U. Kils, "The swimming behavior, swimming performance and energy balance of Antarctic krill, *Euphausia superba*," *BIOMASS Sci. Ser.* **3**, 122 pp. (1981).

⁹K. G. Foote, "Linearity of fisheries acoustics, with addition theorems," *J. Acoust. Soc. Am.* **73**, 1932-1940 (1983).